DOI: 10.6060/mhc245884a

Influence of Substitution Patterns in a Set of BODIPY Derivatives on Aggregation Properties in Binary Solvent Mixtures

Elena V. Antina,[a] Daniil D. Gryaznov,[b] Evgeniy E. Molchanov,[b,c] Valeria A. Kalinkina,[a,b] Alexander A. Kalyagin,[a] Tatiana V. Kokurina,[b] Lubov A. Antina,[a] Ksenia V. Ksenofontova,[b,c] Yuriy S. Marfin,[c] and Sergey D. Usoltsev[b,c@]

[a]*G.A. Krestov Institute of Solution Chemistry of the Russian Academy of Sciences, 153045 Ivanovo, Russia*
[b]*Ivanovo State University of Chemistry and Technology, 153000 Ivanovo, Russia*
[c]*Pacific National University, 680035 Khabarovsk, Russia*
[@]*Corresponding author E-mail: sergeyusoltsev@yahoo.com*

Set of five BODIPY fluorescent molecular sensors with various structure was investigated in aqueous mixtures of organic solvents (tetrahydrofuran, dimethylsulfoxide and acetonitrile). It was shown that aggregation behavior in a row of studied compounds is susceptible even to slight structural alterations, such as e.g. heteroatom position. Hydroxyl moieties in investigated compounds provoked intense sensory response to water content in tetrahydrofuran and acetonitrile, reaching 80% quenching within 0 – 10 Vol.% water in mixture. Choice of binary solvent mixture also severely affects spectroscopic callback during aggregation process. It was found that water contents in binary mixtures closely resemble long-known data on formation of micro nonhomogeneities in the corresponding mixtures. In case of meso-vanilin-BODIPY derivative, investigation of fluorescence decays allowed us to graphically demonstrate nonhomogeneity of a water – THF mixture around 75 – 85 Vol. % of aqueous phase. Formal analysis of spectroscopic properties of phosphors in binary solvent mixtures suggest, that specific solvent interactions could be separated from aggregation effects.

Keywords: BODIPY, aggregation, TCSPC, binary solvent mixtures, quenching.

Влияние закономерностей замещения в ряду производных BODIPY на агрегационные свойства в смесях бинарных растворителей

Е. В. Антина,[a] Д. Д. Грязнов,[b] Е. Е. Молчанов,[b,c] В. А. Калинкина,[a,b] А. А. Калягин,[a] Т. В. Кокурина,[b] Л. А. Антина,[a] К. В. Ксенофонтова,[b,c] Ю. С. Марфин,[c] С. Д. Усольцев[b,c@]

[a]*Институт химии растворов им. Г.А. Крестова РАН, 153045 Иваново, Россия*
[b]*Ивановский государственный химико-технологический университет, 153000 Иваново, Россия*
[c]*Тихоокеанский государственный университет, 680035 Хабаровск, Россия*
[@]*E-mail: sergeyusoltsev@yahoo.com*

Набор из пяти флуоресцентных молекулярных сенсоров BODIPY с различной структурой был исследован в водных смесях органических растворителей (тетрагидрофуран, диметилсульфоксид и ацетонитрил). Было показано, что агрегационное поведение в ряду изученных соединений подвержено даже небольшим структурным изменениям, таким как, например, положение гетероатома. Гидроксильные фрагменты в исследованных соединениях вызывали интенсивный сенсорный ответ на содержание воды в тетрагидрофуране и ацетонитриле, достигая 80% гашения в пределах 0–10 об.% воды в смеси. Выбор бинарной смеси раствори-

телей также сильно влияет на спектроскопический обратный вызов во время процесса агрегации. Было обнаружено, что содержание воды в бинарных смесях очень похоже на давно известные данные об образовании микронеоднородностей в соответствующих смесях. В случае производного мезованилина-BODIPY исследование затухания флуоресценции позволило нам графически продемонстрировать неоднородность смеси вода – ТГФ около 75–85 об.% водной фазы. Формальный анализ спектроскопических свойств фосфоров в бинарных смесях растворителей позволяет предположить, что специфические взаимодействия растворителей можно отделить от эффектов агрегации.

Ключевые слова: BODIPY, агрегация, TCSPC, бинарные смеси растворителей, тушение флуоресценции.

Introduction

Fluorescent sensorics is a sustainably growing research area with big prospective impact in practically all branches of science.[1-4] Among the other kinds of sensors, fluorescent molecules stand apart because of their ease of manufacturing and precise response tunability. Boron dipyrrinates (BODIPY) are bright examples of small molecules with typically large quantum yields, molar extinction coefficients, and stability towards photodegradation.[5,6] There is a broad set of substituents known to induce specific sensory response,[7-10] so investigations of BODIPY dyes and other phosphors nowadays tend to be more application-oriented.[11-14] There are however large fundamental challenges to get fluorescent sensors and probes with well-predictable response to mass production. One of the most prominent factors affecting overall fluorescent response of the dye is aggregation.[15,16] With shift in concentration or properties of the environment, fluorescent response of the dyes typically alters due to manifestation of aggregation-induced emission (AIE), aggregation-caused quenching (ACQ), formation of excited dimers (excimers), hindered twisted intramolecular charge transfer (TICT) or other effects.[17,18,19] And most notably, observed changes are emergent in their nature, so that aggregation in different media could lead to various spectroscopic outcomes.

One of the most popular approaches towards investigation of aggregation properties of fluorescent dyes is a spectroscopic investigation in a series of binary solvent mixtures (with one of the components being water). Very little if any attention is usually put into the way in which the solvent mixture itself affects aggregation properties, and solvent mixtures are usually assumed interchangeable. Among the most widely used components in aqueous–organic mixtures, tetrahydrofuran (THF), acetonitrile (ACN) and dimethylsulfoxide (DMSO) are to be specifically mentioned. It is long known that properties of these binary solvent mixtures deviate from ideal due to specific solvent-solvent interactions at certain concentrations. Water–THF mixtures tend to form nanoscopic heterogeneities, detectable via *e.g.* small-angle neutron scattering (SANS), x-ray scattering, or viscosity measurements.[20-22] Heterogeneities in water–ACN mixtures were also detected with a set of sophisticated methods, such as SANS, picosecond spectroscopy, and with neutron diffraction.[23-26] Finally, water–DMSO mixtures were also proved to be non-ideal via Fourier-transform infrared (IR) spectroscopy and femtosecond IR measurements.[27,28]

Even though these peculiarities are similar in nature, they are known to manifest at different relative concentrations and are usually described in different terms, since labile solvent-solvent structures are extremely hard to investigate. In this paper we attempt to leverage properties of these binary solvent mixtures to further describe emergent fluorescent properties of BODIPY dyes during aggregation in these media.

meso-Aryl substituted BODIPYs are prone to formation of J-aggregates.[29,30] In this work, we studied dyes functionalized in both *meso*- and α-positions. All of the studied compounds bear moieties, susceptible to interactions which grant plausible sensory response. Two *meso*-pyridine-substituted dyes with different heteroatom location were utilized to assess significance of small structural alterations, *meso*-vanilin-substituted BODIPY and α-hydroxystyryl-BODIPY bear hydroxyl moiety in different positions whereas α-pyrrolyl-BODIPY bears heterocyclic NH group. Moreover, two of the compounds, α-hydroxystyryl- and α-pyrrolyl-BODIPY, have batochromically shifted electronic absorption and fluorescence maxima, making them highly prospective for *in vivo* applications. Investigations of these compounds during provoked aggregation in binary solvent mixtures are especially important, since molecular sensors are often utilized in mostly aqueous physiological media, where dyes are extremely prone to aggregation.

Experimental

meso-para-Pyridine-BODIPY (BF2-*ms-p*-pyridine-2,6-diethyl-1,3,5,7-tetramethyldipyrromethene) was synthesized as described elsewhere.[31] ^{1}H NMR (Bruker Avance III 500 NMR spectrometer, 500 MHz, $CDCl_3$) δ ppm: 8.76 (d, J = 5.1 Hz, 2H, $–CH_{aryl}$), 7.31 (d, J = 5.2 Hz, 2H, $–CH_{aryl}$), 2.52 (s, 6H, $–CH_3$), 2.29 (q, J = 7.6 Hz, 4H, $–CH_2–$), 1.29 (s, 6H, $–CH_3$), 0.97 (t, J = 7.6 Hz, 6H, $–CH_3$). MS (Shimadzu AXIMA Confidence MALDI TOF-TOF mass spectrometer) *m/z*: calculated for $C_{22}H_{26}BF_2N_3^+$ $[M]^+$ – 381.22, found – 380.34.

meso-ortho-Pyridine-BODIPY (BF2-*ms-o*-pyridine-2,6-diethyl-1,3,5,7-tetramethyldipyrromethene) was synthesized as described elsewhere.[32] ^{1}H NMR (Bruker Avance III 500 NMR spectrometer, 500 MHz, $CDCl_3$) δ ppm: 8.76 (d, J = 4.7 Hz, 1H, $–CH_{aryl}$), 7.83 – 7.79 (m, 1H, $–CH_{aryl}$), 7.44 – 7.38 (m, 2H, $–CH_{aryl}$), 2.52 (s, 6H, $–CH_3$), 2.28 (q, J = 7.7 Hz, 4H, $–CH_2–$), 1.19 (s, 6H, $–CH_3$), 0.96 (t, J = 7.6 Hz, 6H, $–CH_3$). MS (Shimadzu AXIMA Confidence MALDI TOF-TOF mass spectrometer) *m/z*: calculated for $C_{22}H_{26}BF_2N_3^+$ $[M]^+$ – 381.22, found – 381.46.

meso-Vanilin-BODIPY (BF2-*ms*-phenyl-2,6-diethyl-1,3,5,7-tetramethyldipyrromethene) was synthesized as described elsewhere.[33] ^{1}H NMR (Bruker Avance III 500 NMR spectrometer, 500 MHz, $CDCl_3$) δ ppm: 7.02 (d, J = 8.3 Hz, 1H, $–CH_{aryl}$), 6.77 (d, J = 6.6 Hz, 2H, $–CH_{aryl}$), 3.86 (s, 3H, $–O–CH_3$), 2.52 (s, 6H, $–CH_3$), 2.30 (q, J = 7.6 Hz, 4H, $–CH_2–$), 1.37 (s, 6H, $–CH_3$), 0.98 (t, J =7.6 Hz, 6H, $–CH_3$). MS (Shimadzu AXIMA Confidence

MALDI TOF-TOF mass spectrometer) *m/z*: calculated for $C_{24}H_{29}BF_2N_2O_2^+$ $[M]^+$ – 426.23, found – 426.81.

α-Hydroxystyryl-BODIPY (BF2-*ms*-phenyl-5,5′-bis[2-(4-hydroxyphenyl)ethylenyl]-3,3′-dimethyl-2,2′-dipyrromethene). Mass spectrum *m/z*: 513.61 $[M-F]^+$; 532.64 $[M]^+$. Elemental analysis: Calculated %: C 74.45; H 5.11; N 5.26. $C_{33}H_{27}BF_2N_2O_2$ Found: C 74.43; H 5.09; N 5.23

α-Pyrrolyl-BODIPY (BF2-*ms*-phenyl-4,4'-dichloro-5,5'-bis(pyrrol-2-yl)-2,2'-dipyrrolylmethene) was obtained as described elsewhere.[34] ^{1}H NMR (Bruker Avance III 500 NMR spectrometer, 500 MHz, $CDCl_3$) δ ppm: 10.33 (s,, 2H, NH); 7.50–7.61 (m, 5H, H-Ph); 7.44, 7.19, 6.81, 6.48 (s, 4×2H, H-Pir, 3,3′-H) ($CDCl_3$). Mass spectrum, *m/z*: 467.08 $[M+H]^+$.

Electronic absorption spectra of *meso-para*-pyridine-BODIPY, *meso-ortho*-pyridine-BODIPY and *meso*-vanilin-BODIPY were recorded using Avantes (Avantes, Netherlands) modular spectrometer system consisting of Ava-Light-DHC halogen–deuterium light source, AvaSpec-ULS2048CL-EVO-RS spectrometer and QPod 2e cuvette holder. Steady-state fluorescence spectra were recorded with the Varian Cary Eclipse fluorimeter (Agilent, USA). TCSPC curves of the dyes were recorded with the FluoTime 300 spectrometer (PicoQuant, Germany) with an LED PDL500 excitation source. Fluorescence decay curves were analysed either via built-in software methods or using maximum informational entropy method as described in our recent paper.[30]

Electronic absorption spectra of α-hydroxystyryl-BODIPY and α-pyrrolyl-BODIPY solutions were recorded on SM2203 spectrofluorimeter (SOLAR) at T = 25 ± 0.1 °C. TCSPC curves of the dyes were recorded with FluoTime 300 spectrometer (PicoQuant, Germany) with a laser LDH-P-C-500 (PicoQuant) as an excitation source and emission monochromator set to λ_{em}=545 nm. All studies were carried out in 1 cm path length quartz cuvettes.

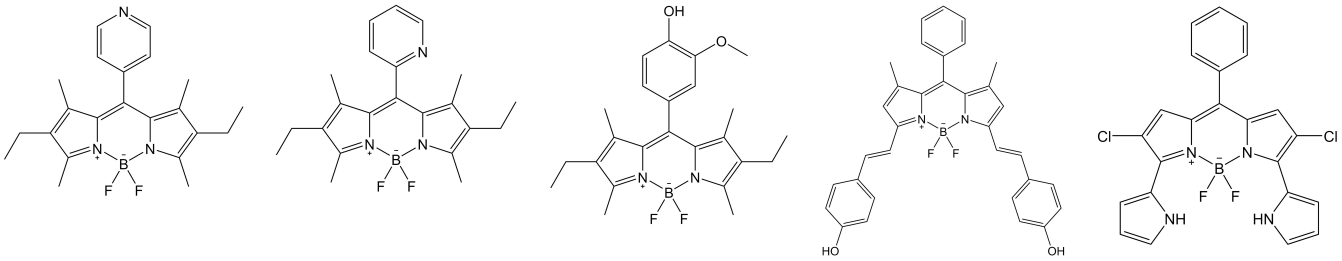

Figure 1. Structures of investigated BODIPY derivatives.

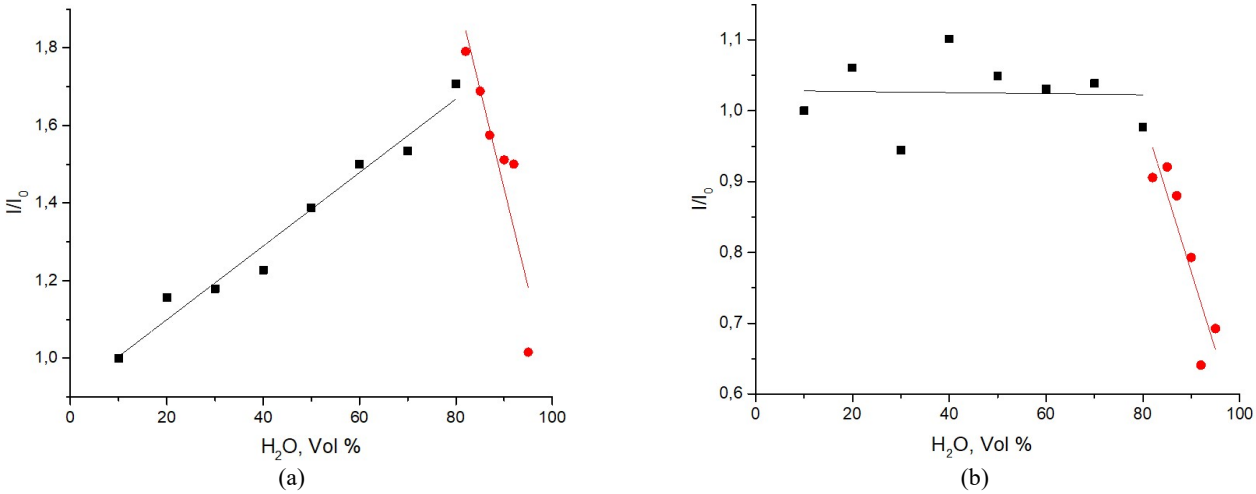

Figure 2. Dependencies of fluorescence intensity on water content for (a) *meso-ortho*-pyridine-BODIPY and (b) *meso-para*-pyridine-BODIPY in water–ACN mixtures. Dependencies are normalized to the first point. Black points are intensities before inflection, red points – beyond "critical" water content. λ_{ex} = 530 nm, λ_{em} = 545 nm for both compounds.

Table 1. Critical points in aggregation process and linear approximation constants of regions before and after inflection in dependency. k_1 and k_2 denote slopes of the lines, describing dependencies of relative fluorescence intensity on aqueous phase concentration (before and after inflection point, correspondingly)

	crit. Vol.% Solv	I_{crit}/I_0	$k_1 \cdot 10^2$	$k_2 \cdot 10^2$
meso-ortho-pyridine-BODIPY Water – ACN	84.6	1.71	0.9	-5.1
meso-ortho-pyridine-BODIPY Water – DMSO	-	-	0.8	-
meso-para-pyridine-BODIPY Water – ACN	78.6	1.02	0	-2.2
meso-para-pyridine-BODIPY Water – DMSO	67.1	0.48	-0.8	0.1

Results and Discussion

Aggregation of meso-substituted BODIPY dyes

Some of the investigated BODIPY dyes (*meso-ortho*-pyridine-BODIPY, *meso-para*-pyridine-BODIPY, *meso*-vanilin-BODIPY) do not demonstrate band-shape alterations in steady-state absorbance spectra, such as *e.g.* formation of *H* or *J* aggregates (example electronic absorption spectra during experiment are presented in ESI, Figure S1). We observe only slight decrease in absorbance intensity during experiment in binary solvent mixture for *meso-ortho*-pyridine-BODIPY and *meso-para*-pyridine-BODIPY, which should be attributed to a low solubility of dyes and their aggregates or their decreased molar extinction (this is not a solvatochromic response, since in that case changes would be monotonic with respect to changes in water content).

Two compounds of similar structure with varying position of heteroatom in *meso*-substituent were investigated in water–DMSO and water–ACN mixtures with varying water content to evaluate impact of very small structural alterations on aggregation properties and solvent response.

Compounds significantly differ in their behaviour in binary mixtures (Figure 2, Table 1, ESI Figure S2). Slopes depend both on compound structure and chosen solvent. It is worth mentioning, that unlike for its' close *meso-para*-pyridine- counterpart, fluorescence intensity for *meso-ortho*-pyridine-BODIPY is growing ($k_1 > 0$) with increase of water content in the investigated data range, meaning that this compound is more predisposed to excited-state interactions with organic solvents of choice (quenched by both DMSO and ACN). Moreover, for *meso-ortho*-pyridine-BODIPY in water–DMSO mixture, there was no change in the observed dependency (no critical point), indicating good suitability of this compound for usage in physiological media. For *meso-ortho*-pyridine-BODIPY in water–ACN and *meso-para*-pyridine-BODIPY in both water–ACN and water–DMSO mixtures, dependency has a sharp inflection point at ratios between 67 and 85 Vol.% of the aqueous part. This range of concentrations of organic phase in binary mixtures is exactly the range in which nonhomogeneities are known to form.

meso-Vanilin-BODIPY was investigated in water–THF mixtures and also assessed in water–ACN mixtures to get alternative results and to distinguish between intrinsic and system-specific properties. Interestingly, in water–THF mixtures this compound demonstrates tremendous quenching response towards water contents within a very small concentration window (0–10% Vol. Water), and also responding to large water content (> 80 Vol.%) with aggregation (Figure 3a). This effectively means that the first solvation shell of the compound may not be the only one driving force of the aggregation process, since two interaction modes in this dependency (quenching by water and aggregation-caused quenching) are situated very far apart in the graph. In water–ACN mixtures (Figure 3b), this compound also demonstrates strong response to water in a very low concentration range, but does not respond to large water quantities like in water–THF mixtures, meaning that quenching caused by water is characteristic for the compound, whereas response happening above 80 Vol.% of water is specific for solvent systems.

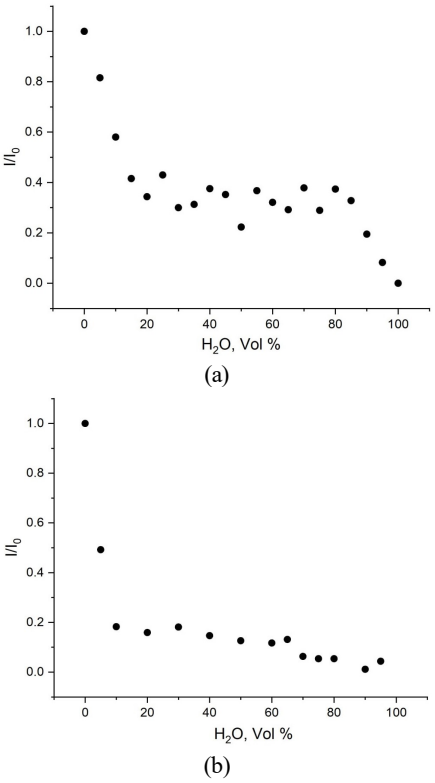

Figure 3. Dependencies of fluorescence intensity on water content for vanilin-BODIPY in (a) water–THF mixtures (λ_{ex} = 480 nm, λ_{em} = 539 nm) and (b) water–ACN mixtures (λ_{ex} = 480 nm, λ_{em} = 537 nm).

From analysis of fluorescence decays via maximum informational entropy method,[30] we were able to extract information about two quenching regions in Water – THF mixtures. Initial increase in water content leads to rapid decrease in the main mode of a lifetime distribution (5 → 1.6 ns, Figure 4a), and this fast lifetime distribution persists until 65 Vol.% of water. With further increase of water content, the lifetime profile evolves to a broad distribution around 2 ns at 80 Vol.% of water, and later sharply decreases to barely analysable short lifetimes, characteristic for water-bound phosphors (Figure 4b).

Recovered lifetime distributions are providing especially interesting insights if we consider BODIPY dye a probe of the environment in a mixture. We see, that solvation environment of a BODIPY remains basically intact in the 20–65% water range (coincidentally with no changes in fluorescence intensity), and after that, we observe micro nonhomogeneity region, earlier found experimentally for water–THF mixtures (in the range of 20–40 Vol.% of THF in water). Further quenching after this point happens due to prevailing dye-water interactions.

This pattern does not manifest itself in water–acetonitrile mixtures (Figure S3), we can still see early decrease in the main lifetime mode up to 10–20%, but consequent quenching is not preceded by nonhomogeneous region, either because water–ACN structures are significantly different in their properties as compared to water–THF, or because singular dye–solvent interactions overcome ensemble early in the quenching process. Probably, solvent interactions are being more pronounced in that case, since absorbance starts to decrease at expected point of approximately 70 Vol. % (Figure S4).

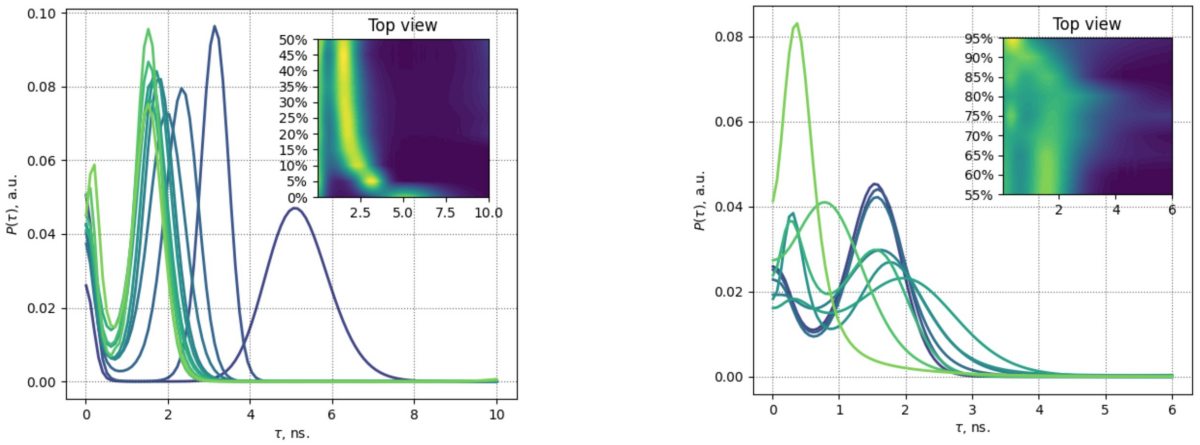

(a) (b)

Figure 4. Fluorescence lifetime distributions obtained from maximum entropy fitting of 100 lifetimes in water–THF mixtures for vanilin-BODIPY in (a) range of 0–10 ns up to 50 Vol.% water content and (b) range of 0–6 ns with water content in the range of 55–95 Vol.%.

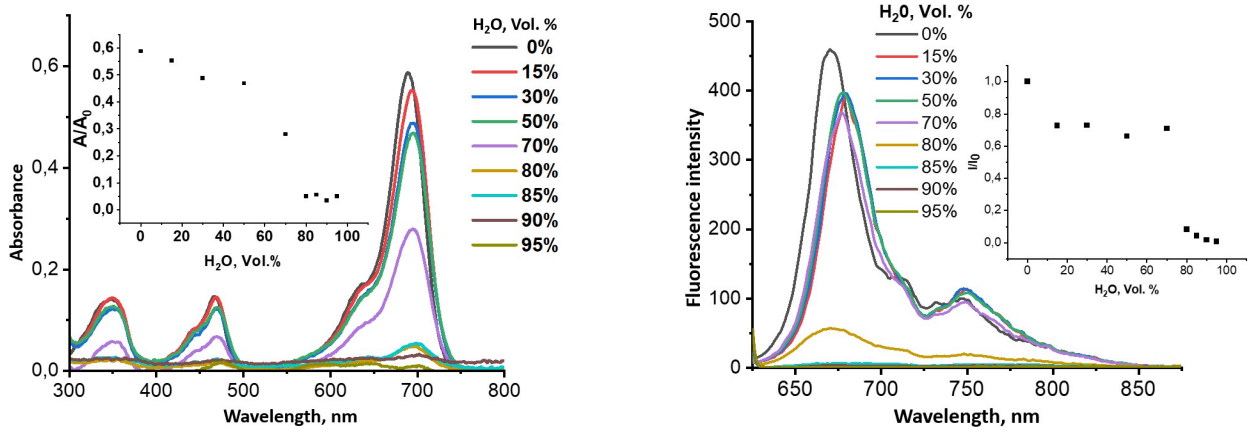

(a) (b)

Figure 5. Absorption (a) and fluorescence (b) spectra of α-hydroxystyryl-BODIPY in THF–water mixtures with varied volumetric water content at a constant dye concentration (C = 6.5 μM); dependence of α-hydroxystyryl-BODIPY absorption (at λ_{abs} = 643 nm) and fluorescence intensity (λ_{em} = 670 nm) to volumetric water content in THF–water mixture, λ_{ex} = 630 nm.

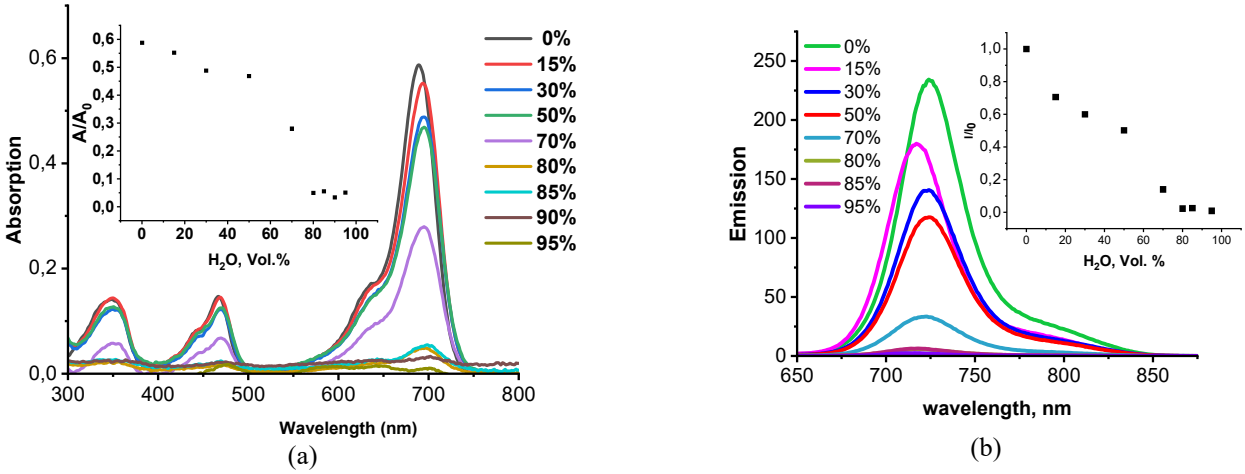

(a) (b)

Figure 6. Absorption (a) and fluorescence (b) spectra of α-pyrrolyl-BODIPY in THF–water mixtures with varied volumetric water content at a constant dye concentration (C = 6.5 μM); dependence of α-hydroxystyryl-BODIPY absorption (at λ_{abs} = 689 nm) and fluorescence (λ_{em} = 725 nm) intensity *vs*. volumetric water content in THF–water mixture, λ_{ex} = 640 nm.

Aggregation of α-substituted BODIPY dyes

Unlike three previously described objects, hydroxystyryl- and pyrrolyl-substituted BODIPY dyes are functionalized in both *meso*- and α-positions. Introduced modifications shift their absorption and fluorescence bands to the near-IR region aka "Phototherapeutic window". Broadened π-electronic structure also provokes strong steady-state interactions, observable in absorption spectra upon increase of water concentration in binary solvent mixtures.

α-Hydroxystyryl-BODIPY (Figure 5) behaves in water–THF mixtures similarly to *meso*-vanilin-BODIPY. The initial drop in fluorescence intensity is less pronounced (30% quenching for *α*-hydroxystyryl-BODIPY *vs*. 60% quenching for *meso*-vanilin BODIPY). Inflection at 70% water content is happening in both dependencies of absorption and fluorescence maxima from water concentration. We assume that similarities of solvatochromic response is due to the fact that both *α*-hydroxystyryl-BODIPY and *meso*-vanilin BODIPY bear hydroxyl moieties in a close proximity of chromophoric systems, leading to possibility of manifestation of photoinduced electron transfer (PET) or resonance energy transfer (RET) provoked by interactions with water molecules (deprotonation of -OH group and weak interactions with water molecules are both plausible).

Whereas for *meso*-vanilin-BODIPY we were unable to definitively attribute quenching after 70% of water to formation of aggregates, changes in spectra of α-hydroxystyryl-BODIPY are characteristic and unambiguous: when the water content increases above 70%, a sharp drop in hydroxystyryl-BODIPY absorption intensity and a 57 nm bathochromic shift of the maximum happens. This spectroscopic behaviour is usually attributed to formation of *J*-type aggregates.

Fluorescence lifetime of α-hydroxystyryl-BODIPY in THF–water mixtures decrease from 4.04 ns in pure THF to 3.5 ns at 70% water content and is properly described by a single exponent. At a water content of 80%, the decay curve is described by a biexponential model (t_{avg} = 3.23 ns) due to formation of ensemble with a fast decay. This fast component was also found for *meso*-vanilin-BODIPY and should probably be attributed to water-solvated fluorophore and its aggregates (thus its low relative intensity). In the THF–water mixture with 95% water content, the average lifetime decreases slightly to 3.04 ns due to increase in relative intensity of fast components. Ensemble becomes highly non-homogenous and the decay curve could only be properly described by a triexponential model (τ_1 – 3.73 ns, τ_2 – 2.4 ns, τ_3 – 0.18 ns). The whole investigated range of Water – THF mixtures demonstrates non-monotonic average lifetime decrease of 25% with increase in water concentration. Aggregated ensembles in mixtures with large water content are especially complicated for investigation via available time-correlated single-photon counting (TCSPC) instrumentation due to very short fluorescence lifetimes of observed species. However, we could still see the common behavior between the investigated dyes in all of the solvent mixtures in a time-resolved regime (*meso*-vanilin-BODIPY in water–THF, water–ACN, α-hydroxystyryl-BODIPY in water–THF). All of the mentioned systems involve poorly resolvable fast components, relative intensities of which are only becoming significant in aqueous media. These fast components are coincidentally manifest with the aggregation process, but should rather be attributed to domination of water in the solvation environment rather than aggregation itself. BODIPY dyes with sensitivity towards water in organic solvents via various mechanisms have been reported before.[35-37] Here we demonstrate how relatively simple structures can respond to water contents just as good or even better than sophisticated molecular architectures.

Dependence of absorption intensities for α-pyrrolyl-BODIPY to water content in water–THF binary mixtures has significantly less pronounced inflection than for all of the investigated compounds, and critical water content in THF–water mixtures is barely recognizable. Fluorescence intensity decreases almost linearly in the investigated range of binary solvent mixtures (Figure 6). When the water content reaches 50%, a smooth decrease of absorption intensity is observed (20% decrease at the main maximum) without any band shape alteration. The most pronounced decrease in the α-pyrrolyl-BODIPY absorption intensity is observed in the 50–80 Vol.% range, and is apparently caused by manifestation of specific dye-solvent interactions and formation of aggregates. Fluorescence is almost completely quenched by 80 Vol.% of water, making further direct investigation of these mixtures via TCSPC non-informative.

Unlike hydroxyl moieties in α-hydroxystyryl-BODIPY and *meso*-vanilin-BODIPY, pyrrolic NH groups in this compound are not prone to interactions with water molecules and observed changes in fluorescence intensities are mostly caused by quenching and aggregation processes.

Conclusions

We demonstrated different interactions in ternary systems of a type BODIPY–Water–Organic solvent. It was found that separation between types of processes during quenching: site-specific solvent interactions, site-independent specific interactions, and aggregational response itself bears significant importance. These processes were found to be distinguishable in case of investigated water–THF mixtures, less pronounced in water–acetonitrile mixtures and almost indistinguishable in water–DMSO mixtures.

First interaction type was deducted from comparison of two compounds with different structure but same responsive moiety: three-modal dependence of fluorescence intensity to water content in a water–THF solution was found both for *meso*-vanilin-BODIPY and α-hydroxystyryl-BODIPY. Quick quenching (up to 80% in 0 – 10% aqueous part) denotes specific interactions of water molecules with hydroxyl moiety of fluorophores, as it was not found for any other investigated compounds.

Second region of dependence should be attributed to non-site-specific interactions, happening due to gradual changes in solvation environment of the dye. These changes are observed as a monotonic change in fluorescence, and were especially graphical for *meso*-*ortho*-pyridine-BODIPY and *meso*-*para*-pyridine-BODIPY. For *meso*-*ortho*-pyridine-BODIPY, before inflection in dependency (at 85 Vol% aqueous part in water–acetonitrile mixture), almost 70% increase in fluorescence intensity is observed.

Last interaction type, as was shown in the paper, aggregation process itself, distinguished by an inflection point on the dependencies in investigated systems with following rapid quenching. Interestingly, it was found that this inflec-

tion happens around the ratios, which were experimentally found to be maximum solvent-solvent interactions regimes elsewhere.

Fluorescence lifetime examination allowed us to demonstrate microscopic nonhomogeneity in water–THF binary mixture as distribution of molecular environment properties around a phosphor. In other solvent mixtures, however, this interesting behaviour was not registered, probably because solvophobic aggregation or water quenching were too severe before water content reached micro nonhomogeneity region.

In practical sense, we should denote that since investigated compounds demonstrate strong response towards water content (in both fluorescence lifetime and fluorescence intensity domains), they could be effectively utilized for analysis of water admixtures in organic solvents.

Acknowledgements. The research was supported by Russian Science Foundation (project No. 22-73-10167).

Author Contributions. Elena Antina: project administration; writing - review & editing. Daniil Gryaznov: investigation. Evgeniy Molchanov: investigation. Valeria Kalinkina: investigation. Alexander Kalyagin: investigation. Tatiana Kokurina: investigation. Lubov Antina: conceptualization, writing - original draft. Ksenia Ksenofontova: investigation, Yuriy Marfin: project administration; funding acquisition. Sergey Usoltsev: conceptualization; writing - review & editing.

References

1. Guo C., Sedgwick A.C., Hirao T., Sessler J.L. *Coord. Chem. Rev.* **2021**, *427*, 213560, DOI: 10.1016/j.ccr.2020.213560.
2. Ushakov E.N., Alfimov M.V., Gromov S.P. *Macroheterocycles* **2010**, *3*, 189–200. DOI: 10.6060/mhc2010.4.189.
3. Lee S.C., Heo J., Woo H.C., Lee J.A., Seo Y.H., Lee C.L., Kim S., Kwon O.P. *Chem. Eur. J.* **2018**, *24*, 13706–13718. DOI: 10.1002/chem.201801389.
4. Haidekker M.A., Theodorakis E.A. *Org. Biomol. Chem.* **2007**, *5*, 1669–1678. DOI: 10.1039/B618415D.
5. Bañuelos J. *Chem. Rec.* **2016**, *16*, 335-348. DOI: 10.1002/tcr.201500238.
6. Poddar M., Misra R. *Coord. Chem. Rev.* **2020**, *421*, 213462. DOI: 10.1016/j.ccr.2020.213462.
7. Loudet A., Burgess K. *Chem. Rev.* **2007**, *107*, 4891–4932. DOI: 10.1021/cr078381n.
8. Boens N., Verbelen B., Ortiz M.J., Jiao L., Dehaen W. *Coord. Chem. Rev.* **2019**, *399*, 213024. DOI: 10.1016/j.ccr.2019.213024.
9. Boens N., Leen V., Dehaen W. *Chem. Soc. Rev.* **2012**, *41*, 1130–1172. DOI: 10.1039/C1CS15132K.
10. Vyšniauskas A., Cornell B., Sherin P.S., Maleckaitė K., Kubánková M., Izquierdo M.A., Vu T.T., Volkova Y.A., Budynina E.M., Molteni C., Kuimova M.K. *ACS Sens.* **2021** *6*, 2158–2167. DOI: 10.1021/acssensors.0c02275.
11. Liu M., Ma S., She M., Chen J., Wang Z., Liu P., Zhang S., Li J. *Chin. Chem. Lett.* **2019**, *30*, 1815–1824. DOI: 10.1016/j.cclet.2019.08.028.
12. Kaur P., Singh K. *J. Mater. Chem. C* **2019**, *7*, 11361–11405. DOI: 10.1039/C9TC03719E.
13. Solomonov A.V., Marfin Y.S., Tesler A.B., Merkushev D.A., Bogatyreva E.A., Antina E.V., Rumyantsev E.V., Shimanovich U. *Colloids Surf. B Biointerfaces* **2022**, *216*, 112532. DOI: 10.1016/j.colsurfb.2022.112532.
14. Koifman O.I., Ageeva T.A., Beletskaya I.P., Averin A.D., Yakushev A.A. *et al. Macroheterocycles* **2020**, *13*, 311–467. DOI: 10.6060/mhc200814k.
15. Descalzo A.B., Ashokkumar P., Shen Z., Rurack K. *ChemPhotoChem* **2020**, *4*, 120–131. DOI: 10.1002/cptc.201900235.
16. Calori I.R., Jayme C.C., Ueno L.T., Machado F.B.C., Tedesco A.C. *Spectrochim. Acta A Mol. Biomol. Spectrosc.* **2019**, *214*, 513–521. DOI: 10.1016/j.saa.2019.02.086.
17. Gao M., Tang B.Z. *ACS Sens.* **2017**, *2*, 1382–1399. DOI: 10.1021/acssensors.7b00551.
18. Xue K., Wang C., Wang J., Lv S., Hao B., Zhu C., Tang B.Z. *J. Am. Chem. Soc.* **2021**, *143*, 14147–14157. DOI: 10.1021/jacs.1c04597.
19. Meng L., Jiang S., Song M., Yan F., Zhang W., Xu B., Tian W. *ACS Appl. Mater. Interfaces* **2020**, *12*, 26842–26851. DOI: 10.1021/acsami.0c03714.
20. Nayak J.N., Aralaguppi M.I., Kumar Naidu B.V., Aminabhavi T.M. *J. Chem. Eng. Data* **2004**, *49*, 468–474. DOI: 10.1021/je030196t.
21. Hao J., Cheng H., Butler P., Zhang L., Han C.C. *J. Chem. Phys.* **2010**, *132*, 154902. DOI: 10.1063/1.3381177.
22. Katayama M., Ozutsumi K. *J. Solution Chem.* **2008**, *37*, 841–856. DOI: 10.1007/s10953-008-9276-0.
23. Takamuku T., Noguchi Y., Matsugami M., Iwase H., Otomo T., Nagao M. *J. Mol. Liq.* **2007**, *136*, 147–155. DOI: 10.1016/j.molliq.2007.02.009.
24. Somnath K., Subhadip G. *ChemPhysChem* **2015**, *16*, 3518–3526. DOI: 10.1002/cphc.201500663.
25. Bakó I., Megyes T., Pálinkás G. *Chem. Phys.* **2005**, *316*, 235–244. DOI: 10.1016/j.chemphys.2005.05.022.
26. Bakó I., Megyes T., Grósz T., Pálinkás G., Dore J. *J. Mol. Liq.* **2006**, *125*, 174–180. DOI: 10.1016/j.molliq.2005.11.022.
27. Oh K.I., Rajesh K., Stanton J.F., Baiz C.R. *Angew. Chem.* **2017**, *129*, 11533–11537. DOI: 10.1002/ange.201704162.
28. Lotze S., Groot C.C.M., Vennehaug C., Bakker H.J. *J. Phys. Chem. B* **2015**, *119*, 5228–5239. DOI: 10.1021/jp512703w.
29. Antina L.A., Ksenofontov A.A., Kazak A.V., Usol'tseva N.V., Antina E.V., Berezin M.B. *Colloids Surf. A Physicochem. Eng. Asp.* **2021**, *618*, 126449. DOI: 10.1016/j.colsurfa.2021.126449.
30. Usoltsev S.D., Raitman O.A., Shokurov A.V., Marfin Y.S. *J. Mol. Liq.* **2023**, *375*, 121380. DOI: 10.1016/j.molliq.2023.121380.
31. Ulrich G., Ziessel R. *J. Org. Chem.* **2004**, *69*, 2070–2083. DOI: 10.1021/jo035825g.
32. Giuffrida M.L., Rizzarelli E., Tomaselli G.A., Satriano C., Trusso Sfrazzetto G. *Chem. Commun.* **2014**, *50*, 9835–9838.
33. Marfin Y.S., Merkushev D.A., Usoltsev S.D., Shipalova M.V., Rumyantsev E.V. *J. Fluoresc.* **2015**, *25*, 1517–1526. DOI: 10.1007/s10895-015-1643-9.
34. Duran-Sampedro G., Agarrabeitia A.R., Garcia-Moreno I., Costela A., Bañuelos J., Arbeloa T., López Arbeloa I., Chiara J.L., Ortiz M.J. *Eur. J. Org. Chem.* **2012**, *2012*, 6335–6350. DOI: 10.1002/ejoc.201200946.
35. Tsumura S., Ohira K., Imato K., Ooyama Y. *RSC Adv.* **2020**, *10*, 33836–33843. DOI: 10.1039/D0RA06569B.
36. Ooyama Y., Hato M., Enoki T., Aoyama S., Furue K., Tsunoji N., Ohshita J. *New J. Chem.* **2016**, *40*, 7278–7281. DOI: 10.1039/C6NJ01467D.
37. Maillard J., Rumble C.A., Fürstenberg A. *J. Phys. Chem. B* **2021**, *125*, 9727–9737. DOI: 10.1021/acs.jpcb. 1c05773.

Received 16.04.2024
Accepted 29.07.2024